ChemComm

COMMUNICATION

View Article Online
View Journal | View Issue

Cite this: *Chem. Commun.*, 2016, 52, 10968

Received 23rd June 2016,
Accepted 8th August 2016

DOI: 10.1039/c6cc05215k

www.rsc.org/chemcomm

Electrochemical synthesis of fractal bimetallic Cu/Ag nanodendrites for efficient surface enhanced Raman spectroscopy†

Da Li,[a] Jingquan Liu,*[b] Hongbin Wang,[d] Colin J. Barrow[c] and Wenrong Yang*[c]

Here, we for the first time synthesized bimetallic Cu/Ag dendrites on graphene paper (Cu/Ag@G) using a facile electrodeposition method to achieve efficient SERS enhancement. Cu/Ag@G combined the electromagnetic enhancement of Cu/Ag dendrites and the chemical enhancement of graphene. SERS was ascribed to the rough metal surface, the synergistic effect of copper and silver nanostructures and the charge transfer between graphene and the molecules.

Surface enhanced Raman spectroscopy (SERS) is a useful analytical technique, which enables sensitive single-molecule detection and provides molecule-specific chemical fingerprints. It takes advantage of the plasmonic resonances in metallic nanostructures to obtain significantly enhanced Raman signals of the adsorbed molecules.[1] In a SERS experiment, a rough metal surface or a colloidal metal nanostructure is typically used. During the past decades, considerable effort has been made to fabricate an ideal SERS substrate with appropriate curved metal regions, giving rise to greatly enhanced local electromagnetic fields *via* the localized surface plasmon resonance effect. The localized electromagnetic field results in the dominant contribution to SERS enhancement *via* the well-known electromagnetic mechanism (EM), which can reach 10^8 or more.[2] In addition to the EM, there is another chemical contribution, called the chemical mechanism (CM), but with a minor enhancement factor of 10–10^2.[3] The CM comes from a charge transfer between the probe molecules and the substrate.[3] An excellent substrate should meet the following three important requirements: a high enhancement factor; uniformity and reproducibility; and facile synthesis.[4] Noble metal nanoparticles have been employed in applications of SERS.[5,6] Gold and silver nanoparticles (NPs) have been widely employed in SERS because of their high SERS activity, and their controllable and variable particle size and shape. Gold NPs are more stable than silver NPs but the SERS enhancement is usually less. However, silver is less stable and more likely to be oxidized when exposed to air.[7] Analogous to Au and other noble metals, copper nanocrystals display strong localized surface plasmon resonance (LSPR). In addition, copper nanocrystals can decrease the cost of noble metals as SERS substrates. Recently, bimetallic dendritic particles, composed of two different metal elements, have been of greater interest than monometallic ones, due to their advantages, including high SERS, high selectivity, and catalytic properties.[8,9] Bimetallisation can improve the performance of the original pure single-metal nanoparticle and create new properties that may not be achieved by monometallic particles.

A number of techniques have been developed in recent years to synthesize noble metal nanoparticles and bimetallic nanoparticles. These include hydrothermal processes in liquid medium,[10] chemical reduction,[11] thermal decomposition of transition-metal complexes[12] and electrochemical synthesis.[13] Unfortunately, most of the methods have some disadvantages, such as the use of surfactants, reducing agents, or toxic organic solvents, which limits their applications in terms of the economic and environmental considerations.[14] The electrodeposition synthesis of metals from a salt solution has brought renewed interest in the old subject of ''dendritic'' growth.[15]

Recently, there were reports on the synthesis of bimetallic nanoparticles with well-defined morphologies, composition and properties.[16,17] Traditionally, the bimetallic dendrites were electrochemically deposited on filter paper or metal substrates, such as copper foil. Graphene, a monolayer of carbon atoms arranged in a honeycomb network, has received considerable attention due to its unique electronic properties, high thermal and chemical stability, large surface area and high electrical conductivity.

[a] *College of Mechanical and Electrical Engineering, Qingdao University, Qingdao 266071, China*
[b] *College of Materials Science and Engineering, Laboratory of Fiber Materials and Modern Textile, The Growing Base for State Key Laboratory, Qingdao University, Qingdao 266071, China. E-mail: jliu@qdu.edu.cn*
[c] *Center for Chemistry and Biotechnology, Deakin University, Waurn Ponds, Geelong, Victoria 3216, Australia. E-mail: wenrong.yang@deakin.edu.au*
[d] *School of Chemistry and Environment, Yunnan Minzu University, Kunming, Yunnan 650500, China*

† Electronic supplementary information (ESI) available. See DOI: 10.1039/c6cc05215k

Graphene provides better dispersion of metal nanostructures on its surface and hastens the electron transfer process.[18] A single-layer graphene has been shown to provide an enormous enhancement effect on the Raman signal intensity.[19] A number of noble metal nanoparticles including Pt, Pd, Au, Ag, and some of their bimetallic combinations have been prepared, and the enhancement can be attributed to the charge transfer between graphene and the molecules. Graphene can be used as a platform for SERS, in which the CM is the dominant cause.[20,21] Inspired by the idea that graphene can act as an efficient SERS substrate, we chose graphene paper as a substrate for electrodeposition of Cu/Ag dendrites and anticipated getting a direct SERS substrate with efficient electromagnetic and chemical effects. To the best of our knowledge, the synthesis of Cu/Ag bimetallic dendrites on a graphene substrate by electrodeposition has not been previously reported.

Herein, for the first time, we synthesized Cu/Ag bimetallic dendrites on graphene paper (Cu/Ag@G) using a co-electrodeposition method without the assistance of a pre-synthesized seed, organic solvent, high temperature or a template. The synthesized Cu/Ag@G showed efficient SERS enhancement (Fig. 1). Our approach has several distinct advantages. Firstly, the synthesis of bimetallic dendrites could be greatly simplified because it does not require multiple steps, such as seed synthesis. Secondly, the rough surface and the synergistic effect of copper and silver nanostructures could greatly contribute to the electromagnetic enhancement and the interaction between the target molecules and graphene should further improve the chemical enhancement, because graphene can accelerate the charge transfer.[22]

The setup for electrodeposition of Cu/Ag on graphene paper (Cu/Ag@G) and a schematic illustration of SERS probe molecules on Cu/Ag@G for SERS are shown in Fig. 1 (for detailed information, please see the ESI†). A fractal deposit was obtained in a circular watch glass with a copper ring anode and a copper wire cathode located in the center. Fractal Cu/Ag@G composites with different atomic ratios of copper to silver were successfully prepared at a potential of 4.0 V. As control experiments, silver, copper or Cu/Ag was also deposited on cotton filter paper instead of graphene paper and the corresponding SERS enhancement was investigated.

The composition of the Cu/Ag@G dendrite was examined by X-ray diffraction (XRD). XRD patterns of bimetallic Cu/Ag@G are shown in Fig. S3a (ESI†). The (111), (200), (220), (311), (222) peaks of cubic Ag indicated the crystalline nature of Ag in the Cu/Ag@G dendrite. Based on the analysis of Cu and Ag, it was found that Cu/Ag@G consists of a purely phase separated bimetallic structure which was consistent with the results of O'Mullane.[23] In addition to Cu and Ag cubic structures, Cu_2O peaks were also observed, which could be attributed to the oxidation of Cu. No shift was observed in the peaks associated with metallic copper and silver, indicating the lack of alloy formation. To further investigate the composition distribution, the dendrites were measured by EDX. As shown in Fig. S3b (ESI†) the EDX spectrum confirmed the presence of Cu and Ag elements in the products. The atomic percentages of Cu and Ag were determined to be 49% and 51%, respectively.

In order to determine the formation process of the dendritic Cu/Ag@G fractals, the samples prepared for different deposition times were monitored using SEM. The representative SEM images of the products prepared at certain reaction time intervals are shown in Fig. 2. The dendrite formation process was proposed and is illustrated in Fig. 3. Ag^+ was reduced first, then Cu^{2+}, to produce dendrites during the reduction process, considering the reduction potentials of Cu^{2+} and Ag^+ ($E_0(Cu^{2+}/Cu)$ = 0.34 V *vs.* SHE; $E_0(Ag^+/Ag)$ = 0.798 V *vs.* SHE). The dendritic structures of the deposits could be controlled *via* a diffusion limited aggregation (DLA) effect.[15] During the electrolysis process, the applied potentials were crucial to the occurrence of deposition of Ag and Cu, since the overpotential was the main electrochemical driving force in the constant potential mode, which significantly

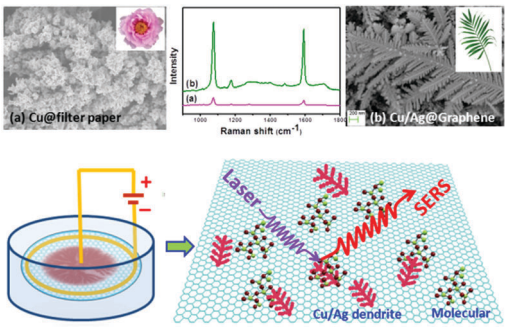

Fig. 1 Schematic setup for the formation of Cu/Ag dendrites on a graphene substrate and SERS probe molecules on Cu/Ag@G for SERS.

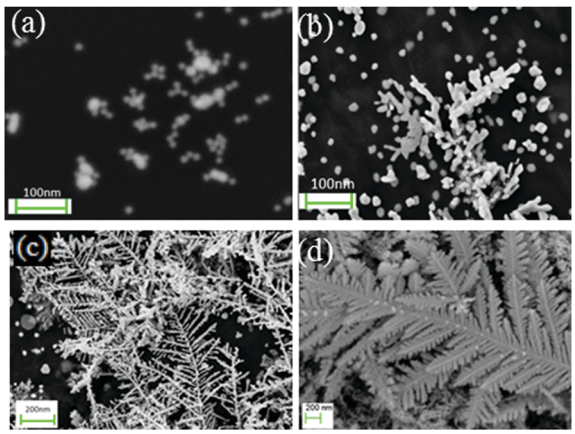

Fig. 2 Representative SEM micrographs of Cu/Ag electrodeposited on graphene paper at a potential of 4.0 V for (a) 1 min, (b) 10 min, (c) 1 hour, and (d) 5 hours.

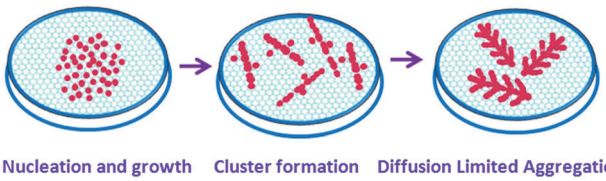

Fig. 3 Schematic illustration of the formation of Cu/Ag dendrites on graphene substrates.

affected the nucleation and growth kinetics. Metal deposition was a process of nucleation and crystal growth.[24]

The time period between the time when the potential was applied and the time when the dendrites began to form was called the incubation period. The incubation on graphene paper was much shorter than that on filter paper. The surface chemistry of graphene made it more suitable as a substrate for deposition than filter paper.[25] The functional groups of graphene, such as the carboxyl groups, are negatively charged. The positively charged metal ions more readily diffused onto the graphene surface due to the electrostatic adsorption associated with the negatively charged graphene surface. There were more sites for nucleation and growth on the graphene surface than on filter paper. Furthermore, the metal ions (Ag^{+}, Cu^{2+}) complexed with graphene and acted as bridges connecting graphene sheets. This binding can be rationalized due to the chemical interaction between the functional groups on graphene and the metal ion. The presence of metal ions in graphene could introduce new energy levels along the electron transport pathway and open up possible conduction channels.[26]

The morphologies of the samples were studied using field-emission scanning electron microscopy (SEM). Fig. S4 (ESI†) shows the SEM images of Cu@G and Cu/Ag@G with different atomic ratios of Ag to Cu. The BET surface area of Cu/Ag@G (Cu : Ag = 1 : 1) was measured using N_2 sorption/desorption measurements and a value of 177 m^2 g^{-1} was calculated. It is much higher than that of graphene (60 m^2 g^{-1}). The high specific surface area was due to the structure of dendrites on graphene. The average size of the Cu/Ag@G (Cu : Ag = 1 : 1) particles is about 50 ± 5 nm. The size measured by dynamic light scattering (65 ± 7 nm) was slightly higher than that obtained using SEM. The shape and size of the nanoparticles were readily controlled by the preparation conditions including the substrates used to deposit, the applied potential, the concentration of Ag^{+} or Cu^{2+}, the atom ratio of Cu and Ag, and the pH of the electrolyte. Fig. S4 (ESI†) shows that the morphology of Cu@G appeared like a flower composed of copper nanoparticles. With increasing silver concentration, the morphology changed from a flower to leaf-like with a main leaf stipe and branches on two sides. The angle between the stipe and the branch was 60°. The overpotential was not only the driving force, but also affected the shape and size of dendrites. When the potential increased from 4.0 V to 5.0 V, the mean size of the dendrites increased and the size became non-uniform (Fig. S5f, ESI†).

Raman spectroscopy was obtained using a Renishaw Raman microscope with three laser lines, 785, 633 and 514 nm (for detailed information, please see the ESI†). The SERS measurements were carried out using 4-mercaptobenzoic acid (4-MBA) as the probe molecules. Typical Raman spectra of MBA with Cu/Ag@G are shown in Fig. 4. We found two intense peaks of the spectra located at 1075 and 1590 cm^{-1}, which were assigned to CH in-plane bending and C–C symmetric stretching vibrations from 4-MBA. Fig. 4a shows that the SERS intensities on Cu@G, Ag@G and Cu/Ag@G were much higher than those on filter paper, respectively. The relative Raman intensities of

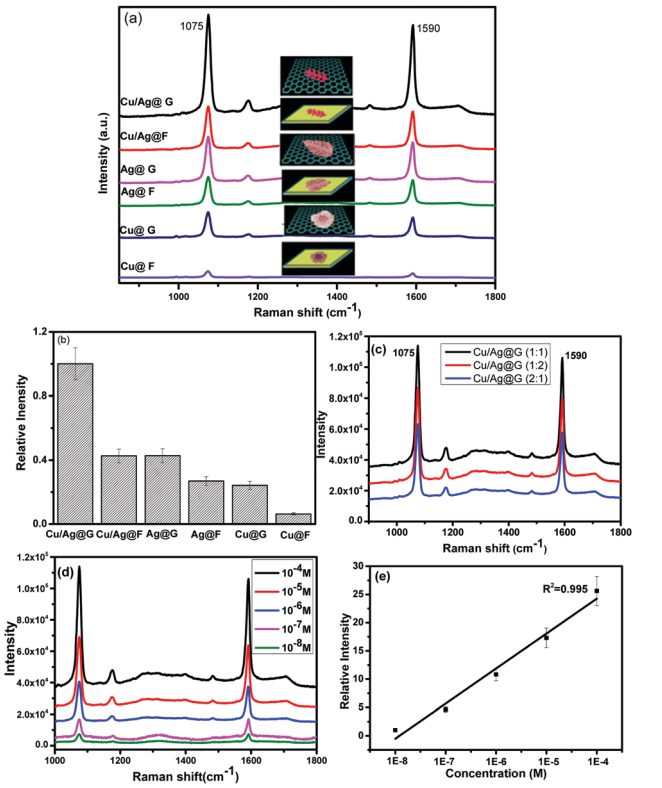

Fig. 4 (a) The SERS spectra of 4-MBA (10^{-4} M) on Cu/Ag@G, Cu/Ag@filter paper, Ag@G, Ag@filter paper, Cu@G and Cu@G upon 785 nm excitation. (b) The relative intensity of different SERS substrates in (a). (c) SERS spectra of 4-MBA (10^{-4} M) on Cu/Ag@G with different atomic ratios of Cu to Ag upon 785 nm excitation. (d) SERS spectra of 4-MBA with different concentrations on Cu/Ag@G (1 : 1) upon 785 nm excitation. (e) The relative Raman intensity with MBA concentration derived from (d). The peaks for D and G bands of graphene were subtracted.

different Raman substrates are shown in Fig. 4b. The enhancement could be attributed to the charge transfer between graphene and the molecules. Graphene is a one-atom thick sheet of hexagonally arranged carbon and the basic structure of 4-MBA contains a phenyl ring with carboxyl and sulfhydryl functional groups. Because of the similarity of the chemical structure between the molecules and graphene, vibrational coupling between them could be another factor contributing to Raman enhancement. The charge transfer can readily occur between graphene and the molecules, which would induce chemical enhancement. Furthermore, the intensity of Cu/Ag@graphene was higher than those of Cu@graphene and Ag@graphene. The intensity of Cu/Ag@graphene was two times higher than that of Cu/Ag@filter paper and 16 times higher than that of Cu@filter paper. This means that the dendrites deposited on graphene had much more efficient enhancement than those deposited on filter paper. The SERS enhancement of bimetallic dendrites was higher than that of monometallic ones, owing to the synergistic effect of copper and silver. The main purpose of adding Cu in the system is to provide a synergistic effect of Cu and Ag for SERS owing to the electromagnetic coupling.

Cu/Ag@G with a 1 : 1 atomic ratio of Cu to Ag showed the highest SERS enhancement. The signal intensity of 4-MBA on Cu/Ag@G (1 : 1) was nearly 1.5 times higher than that on the other two (Fig. 4c). With the increase of the atomic ratio of silver to copper (from 1 : 2 to 1 : 1), the SERS enhancement increased. This was primarily due to the increasing silver ingredient, since silver is a more active SERS metal. However, the enhancement would decrease when the atomic ratio reached 2 : 1. The increasing content of silver increases the size of Cu/Ag@G, which consequently deteriorated the SERS enhancement efficiency. The reason was that Ag^{+} was easily reduced compared to Cu^{2+} and Ag grew coarse more readily at the same deposition potential. Besides, large enhancement factors are a likely result of plasmon coupling at the interface of copper and silver, which creates large localized electromagnetic fields.[27] The Ag-to-Cu electromagnetic coupling will be affected by the silver to copper ratio, and the synergistic effect will become maximum with a 1 : 1 atomic ratio of copper to silver. This means that the optimal synergistic effect could be achieved when the feed atomic ratio of copper to silver was designed to be 1 : 1. Then we tested the SERS enhancement of Cu/Ag@G with a Cu to Ag ratio of 1 : 1 upon 785, 633 and 514.5 nm excitation (Fig. 4d, e and Fig. S6, ESI†).

Furthermore, we calculated the Raman enhancement factor (EF) of the Cu/Ag@G (1 : 1) substrate. The intensity of the peak at 1590 cm^{-1} of the 4-MBA molecule was chosen for calculating the SERS enhancement factors. All the spectra were acquired under the same conditions. Through the integrated area of the 1590 cm^{-1} peak, the SERS EF of Cu/Ag@G was estimated to be 3.7×10^5 upon 785 nm excitation. The EF based on the 1075 cm^{-1} peak was 2.5×10^5. The enhancement factor of pure graphene using Pc molecules as probes was about 2–17.[28] The Raman intensity was enhanced by a factor of 14 for graphene (GERS), 580 for SERS (Ag) and 755 for GERS (Ag).[19] The enhancement factor for 10^{-5} M of methylene blue adsorbed on Cu/Ag bimetallic nanoparticles was 5.8×10^3.[29] So the enhancement factor obtained in this work was much higher than that obtained for graphene only or other Cu/Ag bimetallic particles. The enhancement factors obtained from different peaks were variable, which implied the presence of chemical enhancement. The magnitudes of the enhancement and wavelength dependent enhancement factors were both consistent with the chemical enhancement mechanism. The chemical enhancements of different vibrational modes were usually dependent on the geometry of the molecules on the surface. This extra enhancement was attributed to the charge transfer between graphene and the attached molecules, which resulted in a chemical enhancement.

In conclusion, we have synthesized bimetallic Cu/Ag dendrites on graphene paper. The bimetallic dendrite exhibited a significant enhancement of SERS. The rough surface and the synergistic effect of copper and silver nanostructures greatly benefited the electromagnetic enhancement and the interaction between the target molecules and graphene improved the chemical enhancement. The methodology could be generalized for the preparation of other bimetallic dendrites for efficiently enhanced SERS.

The authors would like to thank Deakin University for financial support.

Notes and references

1 J. Huang, Y. Zhu, M. Lin, Q. Wang, L. Zhao, Y. Yang, K. X. Yao and Y. Han, *J. Am. Chem. Soc.*, 2013, **135**, 8552–8561.
2 S. Chen, Z. Yang, L. Meng, J. Li, C. T. Williams and Z. Tian, *J. Phys. Chem. C*, 2015, **119**, 5246–5251.
3 X. Jiang and A. Campion, *Chem. Phys. Lett.*, 1987, **140**, 95–100.
4 K. Jung, J. Hahn, S. In, Y. Bae, H. Lee, P. V. Pikhitsa, K. Ahn, K. Ha, J. K. Lee and N. Park, *Adv. Mater.*, 2014, **26**, 5923.
5 L. F. Zhang, S. L. Zhong and A. W. Xu, *Angew. Chem., Int. Ed.*, 2013, **52**, 645–649.
6 B. Y. Xia, H. B. Wu, X. Wang and X. W. D. Lou, *Angew. Chem., Int. Ed.*, 2013, **52**, 12337–12340.
7 C. Gao, Y. Hu, M. Wang, M. Chi and Y. Yin, *J. Am. Chem. Soc.*, 2014, **136**, 7474–7479.
8 R. He, Y.-C. Wang, X. Wang, Z. Wang, G. Liu, W. Zhou, L. Wen, Q. Li, X. Wang and X. Chen, *Nat. Commun.*, 2014, **5**, DOI: 10.1038/ncomms5327.
9 C. Chen, Y. Kang, Z. Huo, Z. Zhu, W. Huang, H. L. Xin, J. D. Snyder, D. Li, J. A. Herron and M. Mavrikakis, *Science*, 2014, **343**, 1339–1343.
10 Q. Lu, F. Gao and D. Zhao, *Nano Lett.*, 2002, **2**, 725–728.
11 R. M. Crooks, M. Zhao, L. Sun, V. Chechik and L. K. Yeung, *Acc. Chem. Res.*, 2001, **34**, 181–190.
12 J. Park, B. Koo, K. Y. Yoon, Y. Hwang, M. Kang, J.-G. Park and T. Hyeon, *J. Am. Chem. Soc.*, 2005, **127**, 8433–8440.
13 L. Rodriguez-Sanchez, M. Blanco and M. Lopez-Quintela, *J. Phys. Chem. B*, 2000, **104**, 9683–9688.
14 J. Zhang, K. Li and B. Zhang, *Chem. Commun.*, 2015, **51**, 12012–12015.
15 H. Brune, C. Romainczyk, H. Roder and K. Kern, *Nature*, 1994, **369**, 469–471.
16 J. Ustarroz, J. A. Hammons, T. Altantzis, A. Hubin, S. Bals and H. Terryn, *J. Am. Chem. Soc.*, 2013, **135**, 11550–11561.
17 N. Ortiz and S. E. Skrabalak, *Angew. Chem., Int. Ed.*, 2012, **51**, 11757–11761.
18 D. Li, N. Kong, J. Liu, H. Wang, C. J. Barrow, S. Zhang and W. Yang, *Chem. Commun.*, 2015, **51**, 16349–16352.
19 W. Xu, X. Ling, J. Xiao, M. S. Dresselhaus, J. Kong, H. Xu, Z. Liu and J. Zhang, *Proc. Natl. Acad. Sci. U. S. A.*, 2012, **109**, 9281–9286.
20 Z. Zhang, F. Xu, W. Yang, M. Guo, X. Wang, B. Zhang and J. Tang, *Chem. Commun.*, 2011, **47**, 6440–6442.
21 X. Yu, H. Cai, W. Zhang, X. Li, N. Pan, Y. Luo, X. Wang and J. Hou, *ACS Nano*, 2011, **5**, 952–958.
22 F. Schedin, E. Lidorikis, A. Lombardo, V. G. Kravets, A. K. Geim, A. N. Grigorenko, K. S. Novoselov and A. C. Ferrari, *ACS Nano*, 2010, **4**, 5617–5626.
23 I. Najdovski, P. Selvakannan and A. P. O'Mullane, *RSC Adv.*, 2014, **4**, 7207–7215.
24 B. Rezaei and S. Damiri, *Talanta*, 2010, **83**, 197–204.
25 Z. Liu, J. Liu, D. Li, P. S. Francis, N. W. Barnett, C. J. Barrow and W. Yang, *Chem. Commun.*, 2015, **51**, 10969–10972.
26 A. Mohanty, N. Garg and R. Jin, *Angew. Chem., Int. Ed.*, 2010, **49**, 4962–4966.
27 C. J. Orendorff, A. Gole, T. K. Sau and C. J. Murphy, *Anal. Chem.*, 2005, **77**, 3261–3266.
28 X. Ling, L. Xie, Y. Fang, H. Xu, H. Zhang, J. Kong, M. S. Dresselhaus, J. Zhang and Z. Liu, *Nano Lett.*, 2009, **10**, 553–561.
29 D. Zhang and X. Liu, *J. Mol. Struct.*, 2013, **1035**, 471–475.